

magnetic field strength in the plane of the sky to be $B_{\text{pos}} \approx 5.0 d_{300}^{-1/2}$ mG.

With this estimate of the magnetic field strength, we can compare the properties of NGC1333 IRAS4A derived from our observations to the theoretical predictions. The key parameter that determines whether magnetic fields provide support against gravitational collapse is the mass-to-magnetic flux ratio. Using the formula of (27), we find that the mass-to-magnetic flux ratio is $\approx 1.7 d_{300}^{1/2}$ times the critical value for collapse. Uncertainties persist because of the neglect of the protostellar mass and the use of the plane-of-sky component of the magnetic field, which respectively increase and decrease this ratio. The estimated mass-to-magnetic flux ratio implies that the region traced by the SMA is slightly supercritical, which is what the theoretical models predict for the observed scales (4). This is further supported by the detection of observational signatures of infall motions (26).

These data also show that the magnetic energy dominates the turbulent energy in this source. This is demonstrated through β_{turb} , the square of the ratio of the turbulent line width σ_{turb} to the Alfvén speed V_A . From the expression given by (17), we find that $\beta_{\text{turb}} = 0.02$. Therefore, regardless of whether turbulence played a role in the initiation of the collapse of the parent cloud of NGC 1333 IRAS4A, it seems that at the observed stage of the star formation sequence in this region (the class 0 phase), magnetic fields dominate over turbulence as the key parameter to control the star formation process. Finally, the ratio of the magnetic tension to the gravity force, $f_{\text{tension}}/f_{\text{gravity}}$, demonstrates that gravitational forces are sufficient to cause the observed distortion in the magnetic field. This ratio is proportional to $B^2 D^2 / (R \rho M)$, where R is the radius of curvature of a given magnetic field line and D is the distance of the origin of this field line to the center of symmetry (18). From the south easternmost-modeled line of Fig. 1, we can estimate $R \approx 2.5''$ and $D \approx 1.6''$. Using these numbers and the mass derived from the dust emission, we obtain $f_{\text{tension}}/f_{\text{gravity}} \approx 0.20 d_{300}^{-3}$. This value may be increased by a more accurate model for the magnetic field distribution (which would reduce the residuals and thereby increase the estimated magnetic field) or decreased by including the protostellar mass with the dust mass. Nevertheless, it is clear that the two forces are of similar order, as required.

The axis normal to the dusty envelope (44°) lies between the magnetic field axis (61°) and the main outflow axis (19°) (8). This suggests that when the collapse began, the spin and magnetic axes were not aligned. Could this misalignment be related to the observed formation of a binary system in NGC 1333 IRAS 4A? Studies of collapse in rotating magnetized cores show that fragmentation occurs only in the rotation-dominated cases (when centrifugal

forces dominate over magnetic forces) (28, 29). However, in these cases, if the initial spin and magnetic field axes do not coincide, the resulting magnetic field direction is expected to be substantially different from its original orientation. This is contrary to the conditions in IRAS 4A, where the observed field direction is roughly similar to the larger-scale magnetic field (19). In addition, as a consequence of the misalignment, the magnetic field geometry is predicted to be considerably distorted from the hourglass shape we observe. The current morphology of this object may indicate that the initial magnetic and centrifugal forces were comparable in magnitude (29), allowing fragmentation without substantial rotational distortion of the field.

References and Notes

1. T. Ch. Mouschovias, *Astrophys. J.* **373**, 169 (1991).
2. C. F. McKee, E. G. Zweibel, A. A. Goodman, C. Heiles, in *Protostars and Planets III*, E. H. Levy, J. I. Lunine, Eds. (Univ. of Arizona Press, Tucson, AZ, 1993), pp. 327–366.
3. R. A. Fiedler, T. Ch. Mouschovias, *Astrophys. J.* **415**, 680 (1993).
4. D. Galli, F. H. Shu, *Astrophys. J.* **544**, 243 (1993).
5. F. Nakamura, Z.-Y. Li, *Astrophys. J.* **594**, 363 (2003).
6. D. A. Weintraub, A. A. Goodman, R. L. Akeson, in *Protostars and Planets IV*, V. Mannings, A. P. Boss, S. S. Russell, Eds. (Univ. of Arizona Press, Tucson, AZ, 2000), pp. 247–272.
7. G. Sandell, C. Aspin, W. D. Duncan, A. P. G. Russell, E. I. Robson, *Astrophys. J.* **376**, L17 (1991).
8. M. Choi, *Astrophys. J.* **630**, 976 (2005).
9. N. A. Ridge, S. L. Schnee, A. A. Goodman, J. B. Foster, *Astrophys. J.*, in press (available at <http://xxx.lanl.gov/astro-ph/0601692>).
10. N. R. Minchin, G. Sandell, A. G. Murray, *Astron. Astrophys.* **293**, L61 (1995).
11. M. Tamura, J. H. Hough, S. S. Hayashi, *Astrophys. J.* **448**, 346 (1995).
12. J. M. Girart, R. M. Crutcher, R. Rao, *Astrophys. J.* **525**, L109 (1999).
13. P. T. P. Ho, J. M. Moran, K. Y. Lo, *Astrophys. J.* **616**, L1 (2004).
14. R. Blundell, in *Proceedings of the 15th International Symposium on Space THz Technology*, G. Narayanan, Ed. (Univ. of Massachusetts, Amherst, MA, 2004), pp. 3–15.
15. L. Looney, L. G. Mundy, W. J. Welch, *Astrophys. J.* **529**, 477 (2000).
16. D. P. Marrone, J. M. Moran, J.-H. Zhao, R. Rao, *Astrophys. J.* **640**, 308 (2006).
17. S.-P. Lai, R. M. Crutcher, J. M. Girart, R. Rao, *Astrophys. J.* **566**, 925 (2002).
18. D. A. Schleuning, *Astrophys. J.* **493**, 811 (1998).
19. S. Maret, C. Ceccarelli, E. Caux, A. G. G. M. Tielens, A. Castets, *Astron. Astrophys.* **395**, 573 (2002).
20. V. Ossenkopf, Th. Henning, *Astron. Astrophys.* **291**, 943 (1994).
21. A. A. Goodman, P. Bastien, F. Menard, P. C. Myers, *Astrophys. J.* **359**, 363 (1990).
22. S.-P. Lai, R. M. Crutcher, J. M. Girart, R. Rao, *Astrophys. J.* **561**, 864 (2001).
23. M. Houde, *Astrophys. J.* **616**, L111 (2004).
24. S. Chandrasekhar, E. Fermi, *Astrophys. J.* **118**, 113 (1953).
25. E. C. Ostriker, J. M. Stone, C. F. Gammie, *Astrophys. J.* **546**, 980 (2001).
26. J. Di Francesco, P. C. Myers, D. J. Wilner, N. Ohashi, D. Mardones, *Astrophys. J.* **562**, 770 (2001).
27. R. M. Crutcher, *Astrophys. J.* **520**, 706 (1999).
28. M. N. Machida, T. Matsumoto, K. Tomisaka, T. Hanawa, *Mon. Not. R. Astron. Soc.* **362**, 369 (2005).
29. M. N. Machida, T. Matsumoto, T. Hanawa, K. Tomisaka, *Astrophys. J.* **645**, 1227 (2006).
30. The SMA is a joint project between the Smithsonian Astrophysical Observatory and the Academia Sinica Institute of Astronomy and Astrophysics and is funded by the Smithsonian Institution and the Academia Sinica. J.M.G. acknowledges Generalitat de Catalunya and Ministerio de Educación y Ciencia (Spain) for support through grants 2004 BE 00370 and AYA2005-08523. We thank A. A. Goodman, J. M. Moran, and D. J. Wilner for helpful comments.

24 April 2006; accepted 22 June 2006
10.1126/science.1129093

A Long-Period, Violently Variable X-ray Source in a Young Supernova Remnant

A. De Luca,^{1*} P. A. Caraveo,¹ S. Mereghetti,¹ A. Tiengo,¹ G. F. Bignami^{2,3}

Observations with the Newton X-ray Multimirror Mission satellite show a strong periodic modulation at 6.67 ± 0.03 hours of the x-ray source at the center of the 2000-year-old supernova remnant RCW 103. No fast pulsations are visible. If genetically tied to the supernova remnant, the source could either be an x-ray binary, composed of a compact object and a low-mass star in an eccentric orbit, or an isolated neutron star. In the latter case, the combination of its age and period would indicate that it is a peculiar magnetar, dramatically slowed down, possibly by a supernova debris disc. Both scenarios require nonstandard assumptions about the formation and evolution of compact objects in supernova explosions.

RCW 103 is a young (~ 2000 years) shell-type supernova remnant (SNR), with an x-ray point source very close to its center. Since its discovery (1), this source (1E161348-5055, hereafter 1E), characterized by unpulsed, soft x-ray emission and no radio or optical counterpart (2), has been considered a candidate neutron star (NS), obviously young,

assuming that it was born in the same supernova (SN) event that originated the surrounding SNR. Subsequent x-ray observations have shown 1E to have a peculiar temporal behavior, with orders-of-magnitude secular flux variations (3, 4). Variabilities and tentative periodicities for 1E have been proposed in a range from 1 to 6 hours (5–7). At the SNR's distance from Earth

(~ 3.3 kpc), 1E has a luminosity of 10^{33} to 10^{35} erg s^{-1} . Optical and infrared (optical/IR) observations point to an underluminous counterpart for this object: Three faint IR objects, with magnitude $H \sim 22$ to 23, lie in the Chandra error circle (8), but nothing is detected at visible wavelengths (magnitude $R > 25.6$, $I > 25$) (6, 9).

Here we report results obtained during a long uninterrupted observation by the Newton X-ray Multimirror Mission (XMM-Newton) satellite on 23 August 2005, using the positive-negative (10) and metal-oxide semiconductor (MOS) (11) cameras of the European Photon Imaging Camera (EPIC) instrument. The total observing time was 89.2 kiloseconds (ks). Details on data analysis are given in the supporting online material (SOM). In the resulting MOS image of RCW 103 (Fig. 1A), 1E stands out at less than $20''$ from the geometrical center of the remnant, itself $\sim 9'$ in diameter.

Our data show unambiguously that the source is periodic (Fig. 1B). The best estimate of the period (P) is 6.67 ± 0.03 hours (24.0 ± 0.1 ks). The flux modulation is large, with a pulsed fraction (PF) = $43.5 \pm 1.8\%$. A search for fast periodicities was performed, with negative results. Periodicities with $P \geq 12$ ms and $PF \geq 10\%$ are excluded at the 99% confidence level.

As described in the SOM, time-averaged spectra for source and background were extracted for each EPIC detector in the 0.5- to 8-keV range. Single-component models do not yield acceptable results. The best fit is found for a double-component model consisting of a blackbody curve with temperature $kT \sim 0.5$ keV and emitting radius of ~ 600 m, contributing $\sim 70\%$ of the flux, complemented by either a second blackbody ($kT \sim 1$ keV) or a steep power law (photon index $\Gamma \sim 3$) (fig. S1 and table S1). The observed time-averaged flux is 1.7×10^{-12} erg cm^{-2} s^{-1} (0.5 to 8 keV).

The high XMM-Newton throughput and the long observing time yielded a total of 46,900 photons, which provides good enough statistics to allow us to perform phase-resolved spectroscopy. We find evidence for a definite hardening (a higher average photon energy) of the 0.5- to 8-keV spectrum at the peaks of the light curve and a softening at the troughs. Such a spectral evolution may be modeled by a higher temperature and larger emitting area of the dominant blackbody at the peak, coupled to a higher line-of-sight absorption (fig. S2).

The long-term time behavior of 1E before our 2005 observation was also studied and is summarized in Fig. 2. In August 2005, the source

was clearly caught in a low state. We reanalyzed the 50-ks 2001 XMM data, when the source was in a higher state ($\sim 10^{-11}$ erg cm^{-2} s^{-1}). The periodicity seen in 2005 can be recognized (Fig. 2B, upper curve), albeit with a smaller PF ($11.7 \pm 1.4\%$). The period extracted from the 2001 data is 6.72 ± 0.08 hours (24.2 ± 0.3 ks), which is consistent with the 2005 value, with no evidence for a period variation. However, the source phenomenology is completely different. Apart from a factor of ~ 6 difference in the average flux value, the 2001 light curve has a much more complex substructure. The pulsed flux in 2001 is similar to the 2005 one, or $\sim 2 \times 10^{-12}$ erg cm^{-2} s^{-1} . The source time-averaged spectrum is significantly harder than in 2005, with a larger contribution from the high-energy component, as well as a larger absorption (fig. S3 and table S1).

The 6.67-hour periodicity reported here, as well as the long-term flux variability and complex spectral behavior, make 1E unusual among young compact objects still embedded in their SNR and make any interpretation very difficult.

The association of 1E and RCW 103 appears very robust, based on their perfect positional coincidence and on radio studies suggesting consistent distance estimates for the two objects (12). The chance alignment of a foreground object with the center of RCW 103 can be excluded on the basis of the optical data. Although an AM Her system (13) at 50 to 100 pc could show an x-ray phenomenology somewhat similar to the observed one, it would imply an optical/IR counterpart ~ 10 magnitudes brighter. Thus, we will assume that 1E was born together with its host SNR, which is 2000 years old (14).

Interpreting the 6.67 hours as an orbital period, we first explore a binary system hypothesis for 1E, featuring a compact object (either a NS or a black hole) born in the SN explosion and a faint star, for which existing optical/IR data (6, 8, 9) set stringent constraints. The colors and luminosity of the possible counterparts,

assuming an interstellar reddening $A_V \sim 4.5$ (12), are compatible only with a M-class dwarf of ~ 0.4 solar mass (M_\odot) or smaller. 1E would thus be a low-mass x-ray binary (LMXB) that survived the SN event. However, 1E's phenomenology is very unusual for a LMXB. Its highly variable x-ray luminosity ($\sim 10^{33}$ to 10^{35} erg s^{-1}) is low, both compared to the peak luminosities of transient LMXBs ($\sim 10^{38}$ erg s^{-1}) and to the persistent LMXB output (10^{36} to 10^{37} erg s^{-1}). It is a luminosity similar to that of very faint x-ray transients (15), which are, however, very old systems (10^9 years).

Moreover, the pronounced orbital modulation and spectral phase variability reported here have never been observed in LMXBs. The same is true for 1E's long-term evolution, with its dramatic orbital modulation change and long outburst decay (Fig. 2).

Young age could be the explanation. Standard LMXBs are at least hundreds of millions of years older than 1E and have had enough time to evolve (16) to a phase in which the donor star, having filled its Roche lobe, supplies a large mass transfer toward the compact object, via an accretion disc, at a rate close to the Eddington limit. Conversely, in a very young, very-low-mass binary survivor of a SN explosion, a substantial orbital eccentricity is expected (17), with an important role in controlling any mass transfer within the system. For a dwarf star of mass M_d in the range of 0.2 to 0.4 M_\odot , an orbital eccentricity e of 0.5 to 0.2 would position the L1 point just above the dwarf star surface at periastron. Mass exchange would thus become possible within a narrow range of orbital phases, with a transit time of ~ 10 min from the donor through L1 toward the compact object. The transferred material, with its large angular momentum, would start settling in a disc. One also expects substantial orbital modulation in the fraction f of the dwarf star wind mass captured by the compact object. In the Bondi-Hoyle approach (18), $f \propto d^{-2} v_{rel}^{-4}$, where d is the

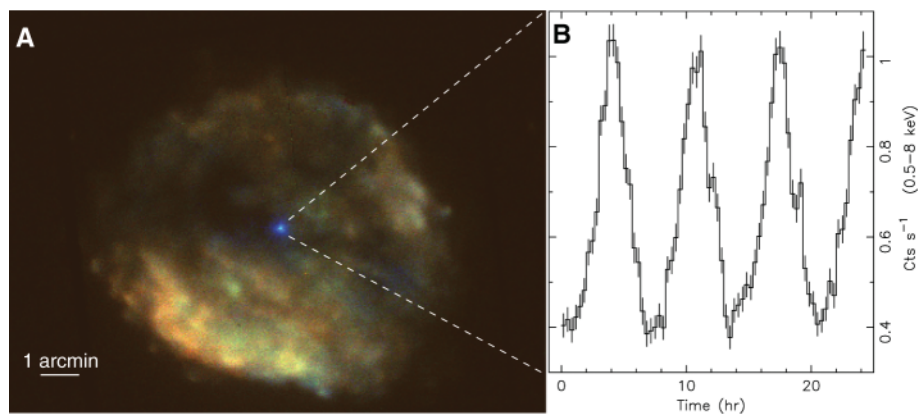


Fig. 1. (A) The young SNR RCW 103 and its central source 1E as observed in August 2005 by the EPIC MOS cameras onboard XMM-Newton. Photon energy is color-coded: Red corresponds to the energy range 0.5 to 0.9 keV, green to 0.9 to 1.7 keV, and blue to 1.7 to 8 keV. North is up, east is left. (B) Background-subtracted flux evolution of 1E in the 0.5- to 8-keV energy range, with its unambiguous 6.67-hour periodicity. Cts s^{-1} , observed counts per second.

¹Istituto Nazionale d'Astrofisica—Istituto di Astrofisica Spaziale e Fisica Cosmica, Via Bassini 15, I-20133 Milano, Italy.

²Centre d'Etude Spatiale des Rayonnements, CNRS-UPS, 9 Avenue du Colonel Roche, 31028 Toulouse Cedex 4, France.

³Dipartimento di Fisica Nucleare e Teorica, Università degli Studi di Pavia, Via Bassi 6, I-27100 Pavia, Italy.

*To whom correspondence should be addressed. E-mail: deluca@iasf-milano.inaf.it

orbital separation and v_{rel} is the relative velocity between the dwarf star wind and the compact object. In 1E, f would vary by a factor ranging from 2.5 to 9 for an M_d of 0.4 to $0.2 M_{\odot}$ and an e of 0.2 to 0.5, with a single peak during the descending part of the orbit, where the combination of velocities is most favorable (fig. S4).

A “double accretion” scenario could thus be at work. Wind accretion provides the bulk of the sharply peaked 6.67-hour modulation, while a disc controls 1E’s long-term variations. Flux outbursts could be due to episodic mass ejections from the dwarf star and/or to disc instabilities, whereas dips in the light curve could be due to occultations by disc structures.

X-ray production remains the crucial point in such a binary model. If the compact object is a NS, accretion can occur if both the rotating dipole (“ejector”) and the centrifugal (“propeller”) barriers (16) can be overcome. The dynamical pressure of the infalling gas must exceed the pressure of the NS dipole radiation, at least down to a distance where corotation with the NS is slower than the keplerian velocity. This would imply that the 2000-year-old NS would have a very low magnetic field and/or a slow rotation period. Indeed, to produce via accretion a luminosity in the range observed for 1E, the above conditions imply (19) $P \sim (0.35 \text{ to } 2.5) B_{10}^{-3/2} \text{ s}$, where B_{10} is the magnetic (B) field in units of 10^{10} G. These values are very peculiar if compared with the canonical picture of a standard 2000-year-old NS, having a B field of a few 10^{12} G and spinning at a few tens of milliseconds. On the other hand, if a black hole is present, accretion processes at the low rates implied by our young binary scenario are expected to be highly inefficient (20), and production of the observed luminosities could be problematic.

Faced with a highly nonstandard binary picture, we also consider an isolated-object scenario for 1E. We focus on NSs, because the periodical modulation rules against a black hole. The 6.67-hour periodicity could be related to the free precession of a fast-rotating NS, with the x-rays coming from a surface hot spot modulated at the precession period (21). However, we find no trace of the expected faster periodicity related to the star rotation. We cannot exclude a peculiar emission geometry, somewhat symmetrical with respect to the rotation axis, but find it an unlikely possibility. Similarly, a NS rotation period shorter than 12 ms seems unlikely, because some evidence of a synchrotron nebula or of nonthermal emission, due to the rotating dipole radiation, would be seen. A nonthermal x-ray output from $\sim 5 \times 10^{34} \text{ erg s}^{-1}$ to $\sim 5 \times 10^{36} \text{ erg s}^{-1}$ is expected (22) for a 12-ms pulsar with a 10^{12} -G B field. Moreover, any precession scenario would not explain the dramatic flux outbursts, together with the other long-term changes in the source phenomenology (Fig. 2).

Alternatively, 1E could be a normal isolated NS, slowly rotating at the 6.67-hour period.

Some huge braking mechanism would have to be invoked to slow it down over 2000 years from its presumably much shorter birth period. To do this with the classical dipole-radiation pulsar mechanism requires the unheard-of, and probably unphysical, magnetic field value of $B \sim 10^{18}$ G. On the other hand, even if 1E were a “normal” NS with a birth period close to 6.67 hours, this would not account for its long-term x-ray flux variability.

1E could, instead, be a magnetar: a neutron star with an ultrahigh magnetic field of the order of 10^{15} G (23), now rotating at 6.67 hours. Indeed, all types of x-ray variabilities observed for 1E, as well as its luminosity and spectral shape, would be naturally explained in the magnetar frame. Magnetar candidates [namely, anomalous x-ray pulsars (AXPs) and soft gamma repeaters (SGRs)] show long-term variations in flux, spectrum, pulse shape, and PF . All magnetars, however, spin more than 1000 times faster than 1E, with periods well clustered in the 5- to 12-s range. The slowing-down mechanism obviously required for 1E could result from the transfer, through its rotating giant B field, of the star’s angular momentum to the material of a hypothetical SN debris disc (a propeller effect). Our detailed calculations (24, 25) show that a disc of $3 \times 10^{-5} M_{\odot}$ would have been enough to slow down, over 2000 years, a $B = 5 \times 10^{15}$ G magnetar, provided it was born with $P \geq 300$ ms (fig. S5). Such a birth period is necessary for avoiding an early ejector phase, because the

pressure of the radiation of the rotating dipole quickly pushes away any disc surrounding a fast magnetar. With a slower rotation at birth, the star instead retains its disc and immediately begins a very efficient loss of rotational energy. A birth period ≥ 300 ms is too long to fit into the most popular explanation (26) for the origin of the huge B fields of magnetars (a dynamo effect in the proto-NS, requiring a birth period of ~ 1 ms). However, alternative high- B -field formation scenarios (such as compression of the progenitor field) have been proposed (27, 28), based on possible evidence that not all magnetars are born as very fast rotators (27).

The recent discovery of a debris disk around an AXP (29) may support a “braked magnetar” picture for 1E, suggesting that at least some magnetars could be surrounded by fossil disks. AXPs and SGRs, as witnessed by their 5- to 12-s periods, did not experience an efficient propeller phase, possibly because of a shorter period at birth or strong gamma-ray bursting activity. If 1E is indeed a slow magnetar, this implies a totally new evolutionary channel for isolated NSs, one in which their spin history is dominated by SN debris. The fraction of NSs following such a channel should be small, however, considering the unusualness of 1E among compact objects associated with SNRs. Furthermore, as for standard AXPs and SGRs, it may be that such objects rapidly (in 10^5 years?) become unobservable. However, one could think of some compact objects not

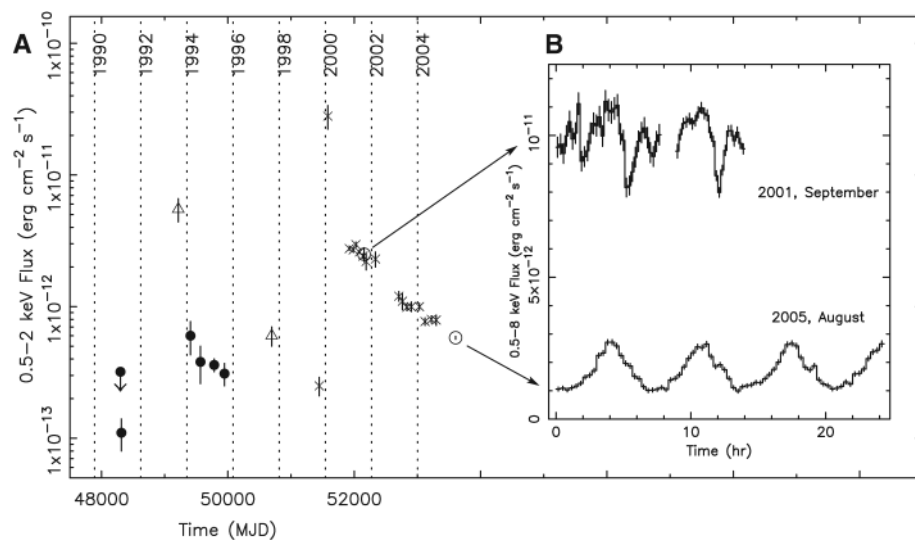


Fig. 2. A synoptic view of time variabilities of 1E. (A) Source secular flux evolution as derived from our analysis of the public Chandra observations (crosses) performed between 1999 and 2005 and two XMM-Newton ones (open circles) performed in 2001 and 2005. A large, two-order-of-magnitude outburst between 1999 and 2000 is followed by a continuous fading down to the level of our 2005 XMM observation. Historical measurements (3) with the Rosat (black solid circles) and ASCA (triangles) satellites are also included and show another episode of flux increase around the ASCA observation in 1993. Source outbursts could thus be recurrent on a several-year time scale. (B) Source flux variation over the 2001 (upper curve) and 2005 (lower curve) XMM-Newton observations, of 50 and 90 ks, respectively. Observation starting times have been aligned, but no folding has been performed. The 6.67-hour periodicity may be seen in the shorter 2001 observation, although with a smaller PF and a much more complex pulse shape.

showing now any pulsation, in spite of large observational efforts, such as sources associated with young SNRs (such as Cas A, Vela Jr, and G347.3-0.4) (6).

Other scenarios could also be explored. We may consider a peculiar binary system in which the 6.67-hour periodicity reflects the spin period of the collapsed object (necessarily a NS), but in which the orbital period is much longer and undetected. As in the isolated NS case, the main difficulty here is to account for a huge braking of the NS rotation in 2000 years, unless it was born spinning at 6.67 hours. As in the case of 2S 0114+650 (30), a binary system featuring a 2.7-hour-period NS and a giant companion with an estimated age of $>10^7$ years, the only viable mechanism could be the propeller effect on the wind of the companion star. Following (19), we note that for plausible parameters of the accretion rate in the 1E system ($\dot{M} \sim 10^9$ to 10^{10} g s $^{-1}$), an equilibrium period of 6.67 hours could indeed result for NS B fields on the order of 10^{12} to 10^{13} G, but the overall NS spin-down process would require 10^8 to 10^{10} years. Assuming instead a magnetar B field of 5×10^{15} G and a higher (but still plausible) accretion rate of 10^{13} g s $^{-1}$, the braking would be much more efficient, but in any case $>20,000$ years would be required to reach a period similar to the observed one. Thus, such a picture seems untenable. One could postulate that 1E and RCW 103 were generated by two different SN explosions within the same binary system, originally composed of two high-mass stars. The first SN produced 1E (at least $\sim 10^5$ years ago, to allow for the fading of the resulting SNR) and did not disrupt the binary. The second produced RCW 103 ~ 2000 years ago but did not leave any visible compact object. 1E could have been slowed down over the lifetime of its companion star ($\sim 10^7$ years?), remaining in any case an active magnetar, as is required to explain its time behavior. Occam's razor argues against such an interpretation. For

a scenario involving a magnetar, the braking of a young isolated object by SN debris seems the most plausible explanation.

Many more details remain to be explored regarding both 1E and RCW 103. Deeper and longer x-ray observations could detect fast pulsations, ruling out the slow rotator model proposed above. Observations during the source's high state could allow for phase-resolved spectroscopy, giving evidence of any intervening circumstellar occulting material. Optical/IR observations could yield the nature of any optical counterpart, to check, for example, on the presence of a disc. It would be also useful to carry out spectral studies of the diffuse remnant material. Although difficult, such studies could be crucial in understanding a SN event that, 2000 years ago, created either a compact object or a binary system so unusual in its physical properties.

References and Notes

1. I. Tuohy, G. P. Garmire, *Astrophys. J.* **239**, L107 (1980).
2. E. V. Gotthelf, R. Petre, U. Hwang, *Astrophys. J.* **487**, L175 (1997).
3. E. V. Gotthelf, R. Petre, G. Vasisht, *Astrophys. J.* **514**, L107 (1999).
4. G. P. Garmire, A. B. Garmire, G. Pavlov, D. N. Burrows, *Bull. Am. Astron. Soc.* **32**, 1237 (2000).
5. G. P. Garmire, G. G. Pavlov, A. B. Garmire, V. E. Zavlin, *IAU Circ.* **7350** (2000).
6. D. Sanwal, G. P. Garmire, A. Garmire, G. G. Pavlov, R. Mignani, *Bull. Am. Astron. Soc.* **34**, 764 (2002).
7. W. Becker, B. Aschenbach, *Proceedings of the 270th WE-Heraeus Seminar on Neutron Stars, Pulsars, and Supernova Remnants*, W. Becker, H. Lesch, J. Trümper, Eds. (Max-Planck-Institut für Extraterrestrische Physik, Garching, Germany, 2002), pp. 64–86.
8. G. G. Pavlov, D. Sanwal, M. A. Teter, in *Young Neutron Stars and Their Environments*, F. Camilo, B. M. Gaensler, Eds. (Astronomical Society of the Pacific, San Francisco, CA, 2004), pp. 239–246.
9. Z.-X. Wang, D. Chakrabarty, in *Neutron Stars in Supernova Remnants*, P. O. Slane, B. M. Gaensler, Eds. (Astronomical Society of the Pacific, San Francisco, CA, 2002), pp. 297–300.
10. L. Strüder *et al.*, *Astron. Astrophys.* **365**, L18 (2001).
11. M. J. L. Turner *et al.*, *Astron. Astrophys.* **365**, L27 (2001).
12. E. M. Reynoso *et al.*, *Pub. Astron. Soc. Australia* **21**, 82 (2004).
13. E. Kuulkers, A. Norton, A. Schwope, B. Warner, in *Compact Stellar X-ray Sources*, W. Lewin, M. van der Klis, Eds. (Cambridge Univ. Press, Cambridge, 2006), pp. 421–460 (available at <http://arxiv.org/abs/astro-ph/0302351>).
14. L. M. Carter, J. R. Dickel, D. J. Bomans, *Proc. Astron. Soc. Pac.* **109**, 990 (1997).
15. A. R. King, R. Wijnands, *Mon. Not. R. Astron. Soc.* **366**, L31 (2006).
16. A. F. Illarionov, R. A. Sunyaev, *Astron. Astrophys.* **39**, 185 (1975).
17. V. Kalogera, *Astrophys. J.* **471**, 352 (1996).
18. K. Davidson, J. P. Ostriker, *Astrophys. J.* **179**, 585 (1973).
19. R. E. Davies, J. E. Pringle, *Mon. Not. R. Astron. Soc.* **196**, 209 (1981).
20. R. Narayan, *Astrophys. Space Sci.* **300**, 177 (2005).
21. J. S. Heyl, L. Hernquist, *Astrophys. J.* **567**, 510 (2002).
22. A. Possenti, R. Cerutti, M. Colpi, S. Mereghetti, *Astron. Astrophys.* **387**, 993 (2002).
23. P. M. Woods, C. Thompson, in *Compact Stellar X-ray Sources*, W. Lewin, M. van der Klis, Eds. (Cambridge Univ. Press, Cambridge, 2006), pp. 547–586 (available at <http://arxiv.org/abs/astro-ph/0406133>).
24. P. Chatterjee, L. Hernquist, R. Narayan, *Astrophys. J.* **534**, 373 (2000).
25. G. J. Franciscelli, R. A. M. J. Wijers, G. E. Brown, *Astrophys. J.* **565**, 471 (2002).
26. R. C. Duncan, C. Thompson, *Astrophys. J.* **392**, L9 (1992).
27. J. Vink, L. Kuiper, *Mon. Not. R. Astron. Soc.* **370**, L14 (2006).
28. L. Ferrario, D. Wickramasinghe, *Mon. Not. R. Astron. Soc.* **367**, 1323 (2006).
29. Z. Wang, D. Chakrabarty, D. J. Kaplan, *Nature* **440**, 772 (2006).
30. X.-D. Li, E. P. J. van den Heuvel, *Astrophys. J.* **513**, L45 (1999).
31. The XMM-Newton data analysis is supported by the Italian Space Agency (ASI) through contract ASI/INAF I/023/05/0. A.D.L. and A.T. acknowledge an ASI fellowship.

Supporting Online Material

www.sciencemag.org/cgi/content/full/1129185/DC1

SOM Text

Figs. S1 to S5

Table S1

References

26 April 2006; accepted 19 June 2006

Published online 6 July 2006;

10.1126/science.1129185

Include this information when citing this paper.

Hexagonal Mesoporous Germanium

Gerasimos S. Armatas and Mercouri G. Kanatzidis*

The blending of mesoporosity with the properties of semiconductors promises new types of multifunctional nanomaterials. It would be particularly interesting to combine the shape selectivity of a mesoporous oxide with the electronic and photonic characteristics of a useful semiconductor. We demonstrated the synthesis of a mesoporous germanium semiconductor using liquid-crystals-templated chemistry. The template removal was achieved by a two-step ion-exchange thermal procedure. This semiconductive mesoporous form of germanium possesses hexagonal pore ordering with very high surface area and exhibits strongly size-dependent optical properties as well as photoluminescence.

The physical and chemical properties of mesoporous (pore size from 20 to 500 Å) solids arise from a well-defined pore structure, high internal surface area, and their framework composition. Mesoporous silicates and transition metal oxides have been extensively

studied for their adsorption, separation, catalytic, and magnetic applications (1–3). Mesoporous carbons, noble metals, and mesostructured organic-inorganic hybrid chalcogenides materials have also been reported (4–12). The pores of a mesostructured material may or

may not be accessible. When the pores become accessible through template removal or otherwise, the system is then defined to be mesoporous. Similar to the silicates, the mesostructured chalcogenides exhibit long-range pore order; however, they have not been rendered porous, and in general attempts to remove the template from the pores result in framework decomposition. Mesoporous semiconductors with well-defined pore structure are relatively unknown materials. Recently, crystalline microporous (pore size < 20 Å) chalcogenides (13) and porous chalcogenide aerogels (14) that possess high porosity have been reported. Porous semiconducting frameworks could exhibit unique properties such as a combination of quantum-

Department of Chemistry, Michigan State University, East Lansing, MI 48824, USA.

*To whom correspondence should be addressed. E-mail: kanatzid@cem.msu.edu